Journal of Science and Technology in Civil Engineering, HUCE, 2026, 20 (1): 30–46

DUAL EFFECT OF FLY ASH ON THE CORROSION RESISTANCE OF LATERAL REINFORCEMENT AND THE STRESS-STRAIN CURVE OF CONFINED CONCRETE

Dung Xuan Le[a], Chinh Van Nguyen[a,*], Paul Lambert[b,c], Quang Hieu Bui[a], Tinh Phuoc Le[a], Loc Van Truong[a], Hiep Van Nguyen[a], Phuong Viet Vu[d]

[a]*Faculty of Civil Engineering, The University of Danang – University of Science and Technology, 54 Nguyen Luong Bang, Danang, Vietnam*
[b]*Sheffield Hallam University, Sheffield, UK*
[c]*Materials & Corrosion Technology, Mott MacDonald, Altrincham, UK*
[d]*Center for Development of Building Technology in Central Region, Vietnam Institute for Building Science and Technology, 61 Le Van Duyet, Son Tra ward, Danang, Vietnam*

Article history:
Received 06/10/2025, Revised 06/01/2026, Accepted 05/02/2026

Abstract

This paper investigates the dual effect of fly ash on the corrosion resistance of lateral reinforcement and stress-strain behavior of confined concrete in reinforced concrete (RC) columns. Twelve columns (150 mm by 150 mm cross-section and 600 mm in height), including four plain (Group 1) and eight RC columns (Groups 2 and 3) were cast with varying fly ash replacement proportions (0%, 10%, 20% and 40%) by weight of ordinary Portland cement (OPC). Lateral reinforcements of Group 2 and 3 were subjected to induce corrosion by an anodic impressed voltage of 3V DC and 6V DC respectively for around 460 hours (19 days). All columns were then tested, and the lateral reinforcement was retrieved to obtain the degree of corrosion. The test results show that the corrosion resistance of the lateral reinforcement was improved significantly when fly ash was used to replace OPC. The corrosion current density passing through lateral reinforcement reduced by more than 80% when 40% of fly ash was used to replace OPC. Under accelerated corrosion, fly ash increases the confinement effect of lateral reinforcement resulting in improvements to the peak stress, corresponding strain at peak stress and ductility of confined concrete. The best improvement in the stress-strain response of confined concrete was when fly ash was used to replace OPC at a proportion of less than 20%. The observed increases were around 10% for peak stress and 92% for strain at peak stress.

Keywords: confined concrete; fly ash; lateral reinforcement; corrosion; stress-strain curve.

https://doi.org/10.31814/stce.huce2026-20(1)-03

1. Introduction

The lateral reinforcement plays an important role in resisting the shear force and enhancing the stress-strain behavior of confined concrete in reinforced concrete (RC) columns through the confinement effect [1, 2]. The transverse reinforcing steel bars restrict the lateral expansion core concrete from expansion resulting in an improvement in strength of confined columns [1, 3–5]. Previous research has shown that the stress-strain response of confined concrete is influenced by a wide range of parameters including type and configuration of lateral reinforcement, concrete compressive strength and cross-sectional geometry. For example, early research concluded that the circular hoops provide double confinement effects compared to the rectangular ties [6]. A wide range of configuration of lateral reinforcement was investigated by many researchers including spirally reinforced columns [7], rectangular ties [8–14] and square ties [3, 15–19].

*Corresponding author. *E-mail address:* nvchinh@dut.udn.vn (Nguyen, C. V.)

Previous research has shown that corrosion of lateral reinforcement has a negative effect on the stress-strain curve of confined concrete. Andisheh et al. [20] conducted an experimental study on twelve full scale circular RC columns and predicted the stress-strain curve of confined concrete when both longitudinal and lateral reinforcement were corroded. They concluded that transverse reinforcement corrosion decreased both the peak stress and strain at the peak stress of confined concrete while also increasing the post-peak slope of the stress-strain curves. Ahmadi et al. [21] stated that the confined concrete strength reduced significantly when lateral reinforcement was corroded by 2.5%. In addition, the corrosion effect was not sensitive to small sized spiral reinforcements. They also proposed a functional relationship between a reduction in compressive strength, corrosion degree and spiral reinforcement diameter. Goharrokhi et al. [22] conducted experimental work and concluded that corrosion percentage, the stirrup diameter and spacing significantly influenced the decrease in concrete strength. Vu et al. [23] concluded that corrosion of transverse reinforcement corrosion negatively influenced the peak stress, corresponding strain at the fracture of the first hoops and descending branch of the stress-strain curves. The authors also proposed a stress-strain curve for confined concrete subjected to corrosion of the lateral reinforcing steel bars based on the well-established Mader et al. model. Zhang et al. [24] also proposed a modified constitutive model for stress-strain characteristics of confined concrete subjected to corrosion of the lateral reinforcement.

Modification of the resultant concrete is one of the effective solutions for increasing the corrosion resistance of reinforcement. OPC is partially replaced by various pozzolanic materials including volcanic ash, silica fume, fly ash, GGBFS, etc. This method reduces the porosity of the cement matrix and increases the concrete resistivity, thereby helping mitigate steel corrosion [25–29]. Fly ash, in particular, is widely used as a supplementary cementitious material due to its economic and performance benefits [30]. While several researcher have investigated the positive effect of fly ash on the reduction in longitudinal reinforcement corrosion [30–35], there is a lack of research on the beneficial influence of fly ash on the corrosion resistance of lateral reinforcement and the stress-strain behavior of confined concrete in RC columns.

This paper presents a comprehensive experimental study into the dual influence of fly ash replacement on the corrosion resistance of lateral reinforcement and stress-strain curve of confined concrete of RC columns. The research method comprises of the use of an anodic impressed voltage for inducing corrosion of lateral reinforcement and evaluate several key parameters including the corrosion current passing through the lateral reinforcements, the degree of corrosion, the surface of corroded lateral reinforcing steel bars, the stress-strain curve of confined concrete, failure modes and cracking patterns of corroded RC columns.

2. Experimental programme

2.1. Test specimens

Four plain concrete columns (Group 1) and eight RC columns (Groups 2 and 3) were tested to evaluate the influence of fly ash on the corrosion prevention of lateral reinforcement and the resultant stress-strain curves of the confined concrete (see Fig. 1 and Table 1). Due to the limitation of laboratory and resources, one specimen per fly ash replacement proportion was used. Each column had dimensions of 600 mm in height and a square cross-section of 150 mm by 150 mm. For each group, OPC was partially replaced by fly ash at the level of 0% (control sample), 10%, 20% and 40% by weight. Three cubes of dimensions $150 \times 150 \times 150$ (mm) were prepared to determine the concrete cube strength.

Groups 2 and 3 samples included four 10 mm diameter longitudinal steel bars and 6 mm diameter lateral reinforcement spaced at 70 mm (Fig. 1). Six lateral reinforcements in each RC columns were

connected to the electrical wires for the accelerated corrosion process. Longitudinal steel bars were insulated from the corroded lateral reinforcements by electrical insulation tape, epoxy and plastic shrink tube prior to casting (see Fig. 2). Strain gauges (5 mm gauge length) were bonded to the longitudinal steel bars for recording the strain during the compression test (see Fig. 1). In order to prevent corrosion damage, strain gauges were covered by epoxy and plastic shrink tube.

Linear variable displacement transducers (LVDTs) were installed on each column side to measure compressive displacement at the confined zone between two embedded stainless-steel bars, 390 mm apart (see Fig. 1). The core concrete strain was calculated by dividing the compressive displacement by the 390 mm gauge length, following previous research [2]. All the columns were cast and cured in the laboratory at 30 °C, RH% 60 for 24 hours, then demolded and water-cured for 28 days before immersion in 3.5% NaCl solution to accelerate corrosion of the lateral reinforcement.

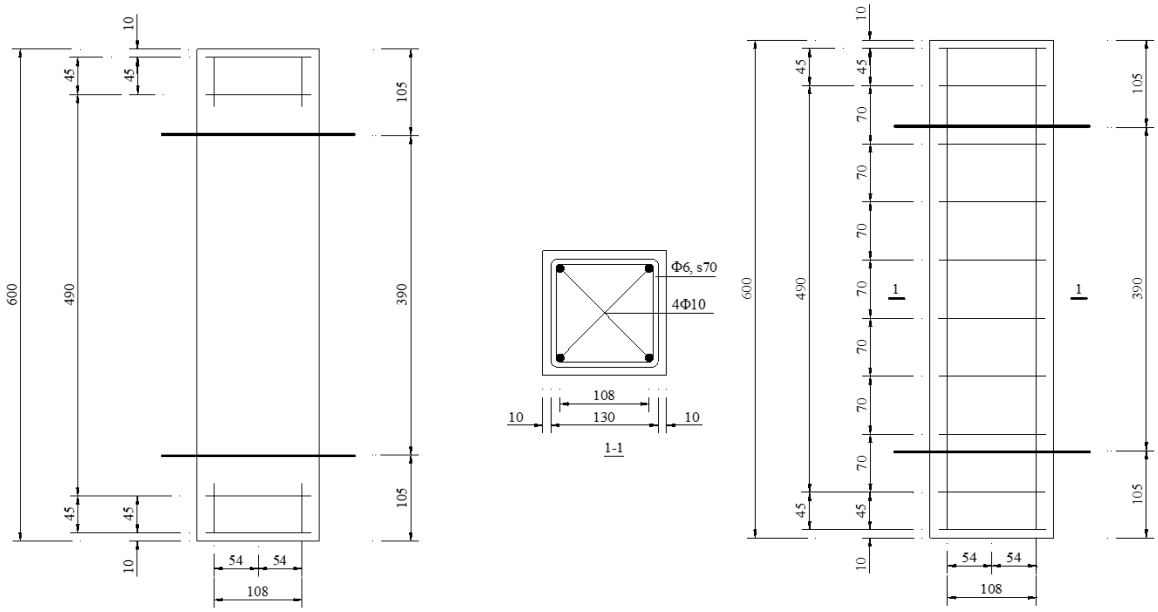

(a) Plain concrete columns (b) RC columns

Figure 1. Details of samples (all dimensions in mm)

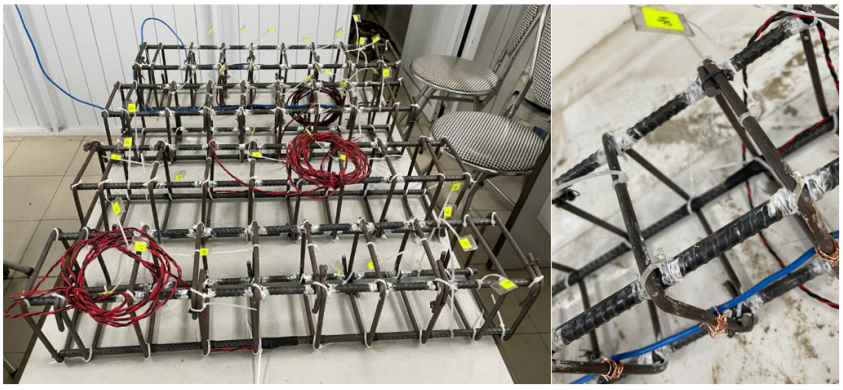

Figure 2. Reinforcing steel cages of RC columns (Groups 2 and 3)

Table 1. Details of test programme

Group	ID	Longitudinal reinforcement	Lateral reinforcement	Fly ash replacement (%)	Constant voltage applied (V)	Compressive cube strength of concrete (MPa)
G1	S0.0.0	–	–	0	–	34.4
	S0.10.0	–	–	10	–	37.6
	S0.20.0	–	–	20	–	38.6
	S0.40.0	–	–	40	–	36.6
G2	S70.0.3	4ϕ10	ϕ6, s70	0	3	34.4
	S70.10.3	4ϕ10	ϕ6, s70	10	3	37.6
	S70.20.3	4ϕ10	ϕ6, s70	20	3	38.6
	S70.40.3	4ϕ10	ϕ6, s70	40	3	36.6
G3	S70.0.6	4ϕ10	ϕ6, s70	0	6	34.4
	S70.10.6	4ϕ10	ϕ6, s70	10	6	37.6
	S70.20.6	4ϕ10	ϕ6, s70	20	6	38.6
	S70.40.6	4ϕ10	ϕ6, s70	40	6	36.6

2.2. Material properties

OPC was obtained from a local supplier in Vietnam. Natural sand and crushed limestone (maximum nominal size 20 mm) was used as fine and coarse aggregate, respectively. The longitudinal and lateral reinforcing steel bars were 10 mm and 6 mm diameter (un-deformed), with yield strengths of 281.1 MPa and 350.7 MPa, respectively. Fly ash was supplied from Vinh Tan power station, Binh Thuan, Vietnam, with its chemical and physical properties listed in Table 2. The total chemical composition of SiO_2 + Al_2O_3 + Fe_2O_3 is more than 70% meeting the requirement of class F fly ash in accordance with TCVN 10302:2014 [36]. Moreover, anhydrous NaCl was added to the mixes at

Table 2. Chemical and physical properties of fly ash

Physical properties	
Fineness (%)	23.5
Loss on Ignition LOI (%)	5.9
Moisture (%)	0.04
Chemical Composition	**Weight (%)**
SiO_2	48.1
Fe_2O_3	17.1
Al_2O_3	15.8
SO_3	0.15
CaO	12.2
MgO	2.18
ZnO	0.01
MnO	0.08
TiO_2	0.69
Na_2O	0.93

3.5% by weight of cementitious material to encourage an accelerated corrosion process. Four concrete mixes with varying fly ash replacement ratios were designed to have high workability with slumps of 6 to 7 cm and presented in Table 3. Compressive cube strengths at the testing age of the RC columns are presented in Table 1.

Table 3. Mix composition of control and fly ash replacement concrete

Mix ID	OPC (kg)	Fly ash (kg)	Sand (kg)	Coarse aggregates (kg)	Water (kg)	NaCl powder (kg)	Slump (cm)
0%FA	22	0	44	66	11	0.77	7
10%FA	19.8	2.2	44	66	10.5	0.77	6
20%FA	17.6	4.4	44	66	10.2	0.77	7
40%FA	13.2	8.8	44	66	9.9	0.77	6

2.3. Accelerated corrosion of lateral reinforcement

At 35 days age (28 days cured in water, and 7 days cured in 3.5% NaCl solution), eight RC columns of Groups 2 and 3 were accelerated corrosion of the lateral reinforcement by using an anodic impressed voltage technique. RC columns were immersed in a tank containing 3.5% NaCl solution with the lateral reinforcement connected to the positive terminal of a direct current (DC) power supply, thereby acting as the anode and corroded. The cathodes are steel rods which were connected to the negative terminal of the DC power supply (Fig. 3). Constant voltages of 3V and 6V were applied to Group 2 and Group 3, respectively. The corrosion process was conducted in the laboratory (28 °C, 60% RH). The 3.5% NaCl solution level was monitored and added manually to compensate for evaporation. An anodic impressed current technique is used to achieve the target degree of corrosion due to the constant current produced. However, in this study, the objective of study is to investigate the effects of fly ash replacement on the corrosion resistance of lateral reinforcement therefore the anodic impressed voltage method was used. The applied voltage was kept constantly resulting in the vary corrosion current density due to the vary resistivity of concrete (with and without incorporating fly ash). The current passing through the lateral reinforcements was continuously recorded.

Figure 3. Inducing corrosion of lateral reinforcement in RC columns

The corrosion acceleration was stopped at around 19 days. The corroded RC columns were removed from solution, cleaned and stored in the laboratory (28 °C, 60% RH). There were no cracks observed along the lateral reinforcing steel bars of the columns.

2.4. Testing of column specimens

At 96 days, twelve columns (including four plain concrete and eight pre-corroded RC) were compressively tested axially at a loading rate of 50 kN/m^2/second. The columns were tested until failure using 100 T capacity universal testing machine. Applied load was recorded by means of a load cell with a nominal capacity of 100 T. The core concrete strain was determined by the ratio of compressive displacement and the distance between two measured points of 390 mm (see Fig. 1). The compressive displacements were recorded by two LVDTs on opposite sides of each column. The LVDT was calibrated by using information supplied by the manufacturer. Both the applied load and displacements from the two LVDTs were recorded by a data logger connected to a computer which was similar to previous research [2] (see Fig. 4).

Figure 4. Testing scheme of twelve columns

2.5. Determination of degree of corrosion of lateral reinforcement

The theoretical and actual degree of corrosion of the lateral reinforcement was determined after completion of testing the RC columns. The theoretical degree of corrosion was computed using Eq. (1) which was widely employed by previous researchers [37–40] based on the mean corrosion current density i (A/cm^2) recorded during the corrosion process.

$$L(\%) = \frac{2 \times 1165 \times i \times T}{D}(\%) \tag{1}$$

where T (years) is the duration of corrosion and D (cm) is the diameter of lateral reinforcement.

The actual degree of corrosion of each RC column was calculated as the mean degree of corrosion of six investigated lateral reinforcing bars using a gravimetric method [37]. Mass loss was determined as the difference between the mass of lateral reinforcement before (m_1) and after corrosion (m_2). The lateral reinforcement was cleaned and weighed before casting the RC columns (m_1). After testing the RC columns, all lateral steel bars were retrieved from the columns by using the hammer, brushed clean after immersing in a proprietary rust removing solution (BO5) for around 24 hours to completely remove the corrosion products. The remaining rust was continuously removed by using fine glass-fibre brush. All lateral reinforcing steel bars were dried and weighed (m_2). The actual degree of corrosion is calculated by using Eq. (2) as the following:

$$L(\%) = \frac{200 \times (m_1 - m_2)}{a \times \gamma \times D}(\%) \tag{2}$$

where γ (7.86 g/cm^3) is the density of steel; a (cm^2) is the surface area of lateral reinforcement before corrosion and D (cm) is the diameter of lateral reinforcement.

3. Results and discussion

3.1. Effect of fly ash on compressive strength of concrete

At 96 days (test age of RC columns), the compressive cube strengths of concrete were 34.4 MPa, 37.6 MPa, 38.6 MPa and 36.6 MPa when OPC was replaced by fly ash at 0% (S0.0.0, S70.0.3, S70.0.6), 10% (S0.10.0, S70.10.3, S70.10.6), 20% (S0.20.0, S70.20.3, S70.20.6) and 40% (S0.40.0, S70.40.3, S70.40.6) by weight, respectively. The concrete cube strength at 96 days increased by 9.3%, 12.2%, 6.4% when OPC was replaced by fly ash at 10%, 20% and 40% (by weight) respectively. The reason for this improvement has been reported by many researchers as the results of the pozzolanic reaction of the high content of SiO_2 in fly ash and the $Ca(OH)_2$ produced from the hydration process of Portland cement and water [41, 42].

3.2. Effect of fly ash on corrosion current densities passing through lateral reinforcement

The applied currents passing through lateral reinforcements of all RC columns were monitored during the accelerated corrosion process and converted to corrosion current density by dividing them by the total surface area of the lateral reinforcement. The corrosion current densities for Group 2 columns (3V DC) and Group 3 columns (6V DC) are shown in Figs. 5 and 6 respectively.

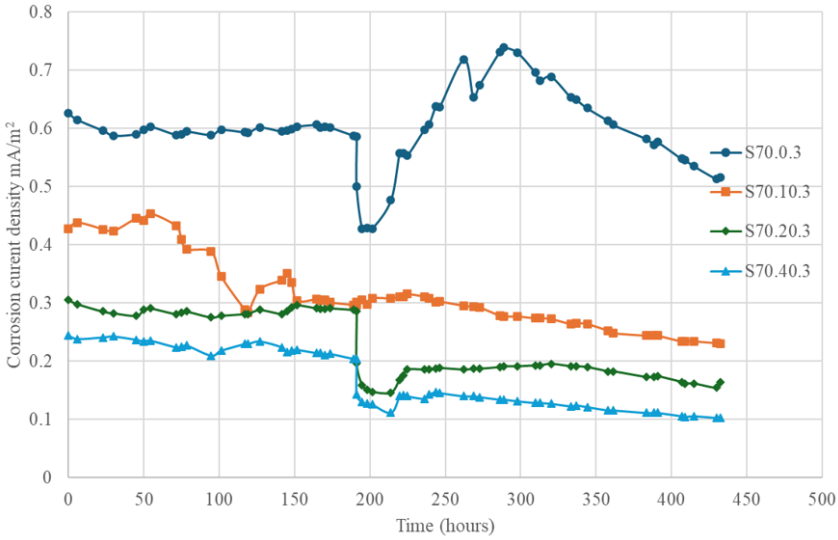

Figure 5. Corrosion current density passing through lateral reinforcement of Group 2 RC columns (3V DC)

Fig. 5 shows that the corrosion current density passing through the lateral reinforcement of Group 2 RC columns (3V DC) decreased as the proportion of fly ash replacement increased, indicating that the corrosion resistance of the lateral reinforcement was increased as a result of the blending of fly ash in concrete. The corrosion current density passing through the lateral reinforcement of the control RC column (0% fly ash) fluctuated from 0.626 mA/cm^2 (total surface area of investigated lateral reinforcement) at the start of the accelerated corrosion process, to 0.516 mA/cm^2 after 432 hours. The corrosion current densities passing through the lateral reinforcement of the 10%, 20% and 40% fly ash replacement RC columns were within the limits of 0.428 mA/cm^2 and 0.230 mA/cm^2; 0.305 mA/cm^2 and 0.164 mA/cm^2; 0.244 mA/cm^2 and 0.102 mA/cm^2, respectively. After 432 hours of accelerating corrosion, the corrosion current density reduced from 0.516 mA/cm^2 for control RC column (0% fly

ash) to 0.102 mA/cm^2 for 40% fly ash replacement RC column, consistent with a reduction of more than 80%. The corrosion current densities passing through the lateral reinforcements within the four RC columns reduced slightly from starting to terminating the accelerated corrosion process. This may be due to the formation of corrosion products around the lateral reinforcement resulting in a change in the resistivity of the concrete.

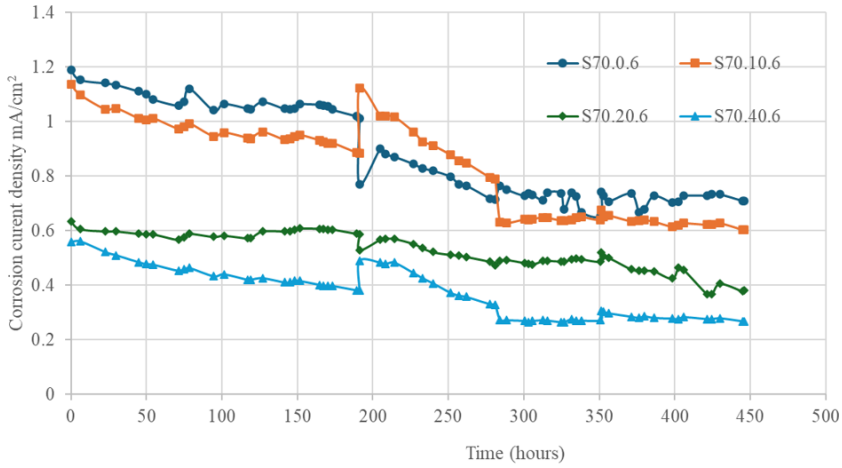

Figure 6. Corrosion current density passing through lateral reinforcement of Group 3 RC columns (6V DC)

Fig. 6 shows that the corrosion current density passing through the lateral reinforcement of Group 3 RC columns (6V DC) decreased as the fly ash replacement ratio increased, similar to Group 2 RC columns. The fly ash again improved the corrosion resistance of the lateral reinforcement at the higher DC voltage of 6V. The corrosion current density passing through the lateral reinforcement of the control RC column (0% fly ash) reduced from 1.19 mA/cm^2 at the start of the accelerated corrosion to 0.71 mA/cm^2 after 466 hours. The corrosion current densities passing through the lateral reinforcement of the 10%, 20% and 40% fly ash replacement RC columns of Group 3 were in the range of 1.137 mA/cm^2 to 0.605 mA/cm^2; 0.633 mA/cm^2 to 0.381 mA/cm^2 and 0.559 mA/cm^2 to 0.267 mA/cm^2 respectively. At 466 hours of accelerated corrosion, the corrosion current density reduced from 0.71 mA/cm^2 for control RC column (0% fly ash) to 0.267 mA/cm^2 for the 40% fly ash replacement RC column, consistent with reduction of more than 62%. For all four RC columns, the corrosion current density passing through the lateral reinforcement decreased from the start to the end of the accelerated corrosion process.

3.3. Surface visual monitoring of corroded lateral reinforcements

The surface of corroded lateral reinforcements of Groups 2 and 3 were visually monitored to study the extent and form of corrosion (see Figs. 7 and 8). In general, the localised corrosion appeared in all lateral reinforcement, the more fly ash replacement the less localised corrosion. This is attributed to the reduction in corrosion current density due to the fly ash replacement. At the higher constant voltage applied of 6V (Fig. 8), the localised corrosion appeared to be clearer than that of 3V DC application (Fig. 7).

It has been noted that the longitudinal reinforcing steel bars remained uncorroded during the corrosion process. The surface of all the longitudinal reinforcing steel bars was the same as before accelerated corrosion (see Fig. 9) demonstrating the effectiveness of the electrical insulation tape.

Figure 7. Surface of lateral reinforcing steel specimens after testing – Group 2 (3V)

Figure 8. Surface of lateral reinforcing steel specimens after testing – Group 3 (6V)

Figure 9. Surface of longitudinal reinforcing steel bars after testing

3.4. Effect of fly ash on the theoretical and actual degree of corrosion of lateral reinforcement

The theoretical and actual degrees of corrosion of the lateral reinforcement are shown in Table 4. The relationships between the fly ash content in RC columns and degrees of corrosion are presented in Fig. 10.

Fig. 10 demonstrates that both theoretical and actual degree of corrosion of the lateral reinforcement reduced when OPC was partially replaced by fly ash. When the fly ash content increases, both theoretical and actual degree of corrosion reduced for Group 2 (3V DC) and Group 3 (6V DC) columns. The actual degree of corrosion is different from the theoretical degree of corrosion for both groups and can be explained by the following reasons. Firstly, there is a difference between the actual and theoretical mass loss based on Faraday's Law. The theoretical mass loss calculated from Faraday's Law is based on general corrosion whereas the actual mass loss was based on localised corrosion on most of the samples in practice (see Figs. 7 and 8) [35, 37, 40]. Secondly, the theoretical mass losses from Faraday's Law is based on assumptions that the amount of charge passed and the type of corrosion products was produced with a valence of iron of 2 (e.g. Fe^{+2}) [37–40]. However, the corrosion products produced in practice and accelerated corrosion process include a range of valences of iron (e.g. Fe^{+2}, Fe^{+3}) depending on oxygen availability.

Table 4. Theoretical and actual degree of corrosion of lateral reinforcement of Group 2 and 3

Group	Beam ID (% fly ash-V DC)	Steel bar ID	Length of steel bar (cm)	Diameter (cm)	Mean corrosion current density (mA/cm^2)	Duration T (years)	Theoretical degree of corrosion (%)	m_1 (g)	m_2 (g)	Actual degree of corrosion (%)	
										Individual	Mean
G2	S70.0.3	1	62	0.6	0.597	0.04934	11.44	123	94	10.53	11.50
		2	62	0.6				123	92	11.25	
		3	62	0.6				122	93	10.53	
		4	62	0.6				125	94	11.25	
		5	62	0.6				123	87	13.07	
		6	62	0.6				123	89	12.34	
	S70.10.3	13	62	0.6	0.313	0.04934	6.0	123	102	7.62	7.38
		14	62	0.6				123	104	6.90	
		15	62	0.6				124	104	7.62	
		16	62	0.6				123	101	7.99	
		17	62	0.6				124	104	7.26	
		18	62	0.6				123	104	6.90	
	S70.20.3	25	62	0.6	0.2241	0.04934	4.29	122	105	6.17	6.47
		26	62	0.6				123	104	6.90	
		27	62	0.6				122	106	5.81	
		28	62	0.6				122	103	6.90	
		29	62	0.6				122	104	6.54	
		30	62	0.6				122	104	6.54	
	S70.40.3	37	62	0.6	0.1676	0.04934	3.21	123	109	5.08	5.31
		38	62	0.6				122	107	5.45	
		39	62	0.6				125	111	5.08	
		40	62	0.6				126	112	5.08	
		41	62	0.6				124	109	5.45	
		42	62	0.6				124	108	5.81	
G3	S70.0.6	7	62	0.6	0.8724	0.05094	17.26	122	81	14.89	15.25
		8	62	0.6				124	79	16.34	
		9	62	0.6				126	82	15.97	
		10	62	0.6				123	83	14.52	
		11	62	0.6				122	81	14.89	
		12	62	0.6				123	82	14.89	
	S70.10.6	19	62	0.6	0.8192	0.05094	16.21	123	87	13.07	11.62
		20	62	0.6				122	88	12.34	
		21	62	0.6				121	94	9.80	
		22	62	0.6				122	92	10.89	
		23	62	0.6				122	94	10.17	
		24	62	0.6				122	85	13.43	
	S70.20.6	31	62	0.6	0.5251	0.05094	10.39	123	98	9.08	9.74
		32	62	0.6				124	97	9.80	
		33	62	0.6				123	98	9.08	
		34	62	0.6				124	94	10.89	
		35	62	0.6				122	98	8.71	
		36	62	0.6				123	93	10.89	
	S70.40.6	43	62	0.6	0.3672	0.05094	7.27	123	100	8.35	8.23
		44	62	0.6				124	100	8.71	
		45	62	0.6				123	101	7.99	
		46	62	0.6				123	102	7.62	
		47	62	0.6				122	99	8.35	
		48	62	0.6				122	99	8.35	

Note: m_1 – measured mass of reinforcing bar before corrosion; m_2 – measured mass of reinforcing bar after corrosion.

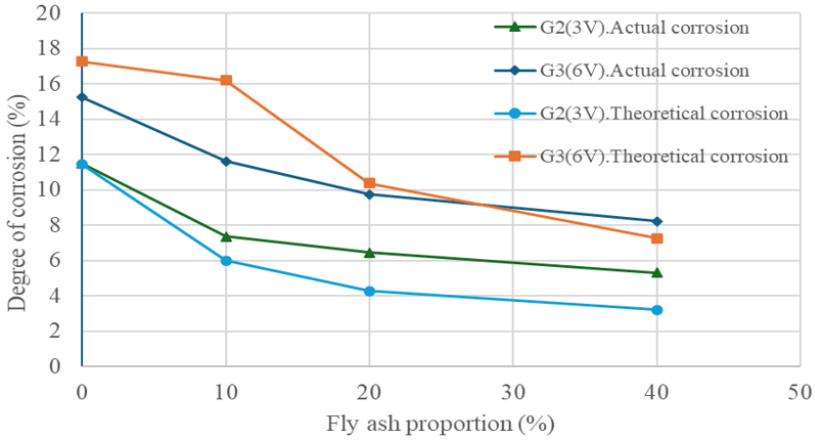

Figure 10. Effect of fly ash on degree of corrosion of lateral reinforcement

3.5. Stress-strain relationship of compressive longitudinal reinforcement

As discussed in Section 3.3, the longitudinal reinforcing steel bars remained un-corroded during the accelerated corrosion process. Therefore, the stress-strain relationship of longitudinal reinforcement were determined by using the modified stress-strain model of Dhaka RP [43] as detailed in previous research [2] and presented in Eqs. (3), (4), (5).

$$\begin{cases} \sigma_{sc} = E_s\varepsilon_{sc}, \quad \varepsilon_{sc} \le \varepsilon_y \\ \sigma_{sc} = \sigma_t\left[1-\left(1-\dfrac{f_i}{f_{it}}\right)\left(\dfrac{\varepsilon_{sc}-\varepsilon_y}{\varepsilon_i-\varepsilon_y}\right)\right] \qquad \varepsilon_y < \varepsilon_{sc} \le \varepsilon_i \\ \sigma_{sc} = f_i - 0.02E_s(\varepsilon_{sc}-\varepsilon_i) \ge 0.2f_y, \quad \varepsilon_{sc} > \varepsilon_i \end{cases} \tag{3}$$

where σ_t is the stress in the tension curve corresponding to ε_{sc} (current strain), f_{it} is the stress in the tension curves corresponding to ε_i (strain at the intermediate point), could be represented by the following Eqs. [43]

$$\frac{\varepsilon_i}{\varepsilon_y} = 55 - 2.3\sqrt{0.01f_y}\frac{L}{D} \ge 7 \tag{4}$$

$$\frac{f_i}{f_{it}} = \alpha\left(1.1 - 0.016\sqrt{0.01f_y}\frac{L}{D}\right) \ge 0.2 \tag{5}$$

where α is a response modifier, $\alpha = 0.75$ for elastic–perfectly plastic bars, $\alpha = 1$ for bars with continuous linear hardening, $\alpha = 0.75 - 1$ for bars with a limited hardening range. L is the restrained length as the lateral reinforcement spacing ($L = s = 70$ mm).

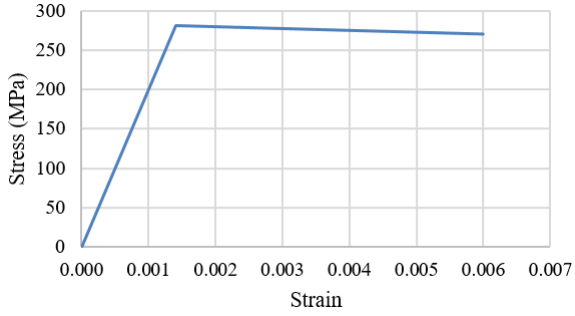

Figure 11. Stress-strain relationship of compressive longitudinal reinforcement within S70.20.3 column (Group 2)

3.6. Effect of fly ash on stress-strain curves of confined concrete under accelerated corrosion

Details of the calculation of stress of confined concrete are described in the previous research [2] and summarized in Eq. (6) as following

$$\sigma_{cc} = \frac{P_{cc}}{A_c(1 - \frac{A_s}{A_c})} \tag{6}$$

where P_{cc} is the load carried by the core of concrete, obtained by subtracting the contributions of concrete cover and longitudinal reinforcement from the total load. It is converted to the core concrete stress by dividing by the core area as shown in Eq. (6) [2, 5, 15]; $A_c = b_c d_c$ is the area of core section enclosed by the centre lines of the lateral reinforcement and A_s is the cross sectional area of longitudinal reinforcement.

The concrete cover was not spalled during the accelerated corrosion process. Therefore, the stress-strain curves of the concrete cover were calculated from the stress-strain curves of the corresponding control samples S0 in Group 1 (S0.0.0, S0.10.0, S0.20.0, S0.40.0). The load carried by the cover concrete of the RC columns is the product of the stress and the cover concrete area [2, 15].

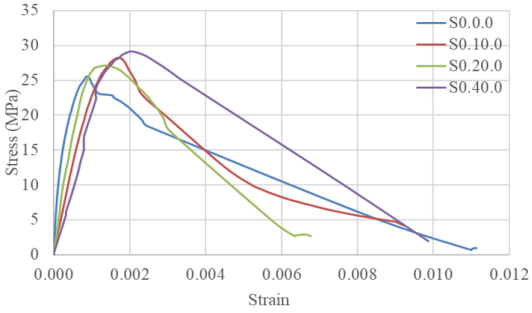

(a) Un-confined concrete (Group 1)

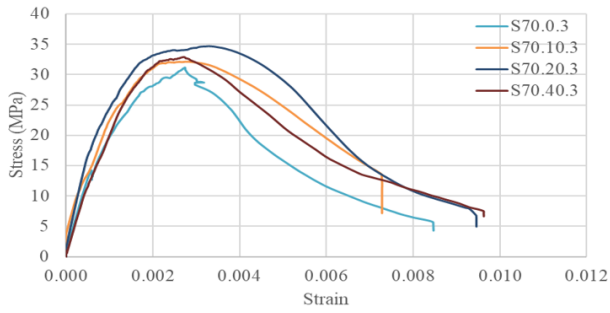

(b) Confined concrete (Group 2)

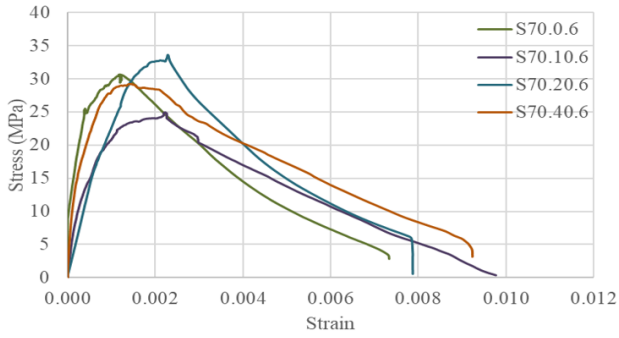

(c) Confined concrete (Group 3)

Figure 12. Stress-strain curves

The stress-strain curves of plain unconfined concrete (G1) and confined concrete subjected to corrosion of the lateral reinforcement (G2 and G3) are shown in Fig. 12. Peak stresses and corresponding strains at peak stresses of the confined concrete are summarised in Table 5. For unconfined concrete (group G1), the locally sourced fly ash increased the peak stress of the confined concrete by 10.5%, 6.1% and 14.0% as fly ash replacement proportions of 10%, 20% and 40%, respectively. The corresponding strain at peak stress of the fly ash concrete was also improved by 92.8%, 54.4% and

131.5% when fly ash was used to replace OPC at 10%, 20% and 40%, respectively. These increases in strain at peak stress may be expected to improve the ductility of the concrete and associated RC members.

Table 5. Summary of peak stress and corresponding strain at peak stresses of unconfined and confined concrete

Group	ID	Compressive cube strength (MPa)	Peak stress (MPa)	Increase in peak stress (%)	Strain at peak stress	Increase in strain at peak stress (%)	Ultimate strain	Stress at ultimate strain (MPa)	Ratio of stress at ultimate strain and peak stress
G1	S0.0.0	34.4	25.6	–	0.000877	–	0.008273	5.6	0.22
	S0.10.0	37.6	28.2	10.5	0.001691	92.8	0.009236	4.2	0.15
	S0.20.0	38.6	27.1	6.1	0.001354	54.4	0.006383	2.8	0.10
	S0.40.0	36.0	29.1	14.0	0.002030	131.5	0.009868	1.9	0.07
G2	S70.0.3	34.4	31.2	–	0.002741	–	0.008461	5.7	0.18
	S70.10.3	37.6	32.1	3.1	0.002808	2.5	0.007284	12.1	0.38
	S70.20.3	38.6	34.7	11.3	0.003292	20.1	0.009303	7.9	0.23
	S70.40.3	36.0	32.9	5.6	0.002711	−1.1	0.009501	7.8	0.24
G3	S70.0.6	34.4	30.7	–	0.001189	–	0.007328	3.2	0.10
	S70.10.6	37.6	24.9	−18.6	0.002230	87.6	0.008633	3.7	0.15
	S70.20.6	38.6	33.6	9.7	0.002285	92.2	0.007862	5.0	0.15
	S70.40.6	36.0	29.2	−4.6	0.001439	21.0	0.009172	4.8	0.17

For Group G2, 3V DC was used for accelerating the corrosion of the lateral reinforcement. Fig. 12(b) and Table 5 show that fly ash improved the stress-strain curves of confined concrete under corrosion attack. After 452 hours of accelerated corrosion, the peak stresses of the confined concrete were 31.2 MPa, 32.1 MPa, 34.7 MPa and 32.9 MPa for the control RC column (S70.0.3, 0%), 10%, 20% and 40%, respectively. In comparison with the control RC column (S70.0.3), the peak stress increased by 3.1%, 11.3% and 5.6% for fly ash replacement of 10%, 20% and 40% fly ash replacement, respectively. The strain at peak stress improved by 2.5% and 20.1% for 10% and 20% fly ash replacement respectively when compared with the control RC columns. However, the strain at peak stress of the 40% fly ash replacement reduced by around 1% in comparison with the control RC column. The improvement of strain at peak stress for the 10% and 20% fly ash replacement samples leads to an improvement in ductility of the confined concrete and RC columns.

For Group G3, a higher voltage of 6V DC was applied for accelerating the corrosion of the lateral reinforcement. Fig. 12(c) and Table 4 show that fly ash also improved the peak stress of the confined concrete when 20% of fly ash was used to replace OPC, whereas there is a slight reduction (4.6%) in peak stress in 40% fly ash samples when compared with the control sample (S70.0.6). The slight reduction in peak stress for S70.40.6 is similar to that of S70.40.3 of Group G2. There is an outlying result of peak stress of sample S70.10.6, apparently due to the uneven surfaces resulting in eccentricity in the RC columns and has been omitted from the general justification. The strain at peak stress for the fly ash samples subjected to corrosion was also improved under the corrosion attacks as it increased by 87.6%, 92.2% and 21.0% when fly ash was used to replace OPC at proportions of 10%, 20% and 40% respectively. The less improvement of peak stress of fly ash samples may be due to the higher voltage application (6V DC) resulting the internal cracking of confined concrete due to the corrosion of lateral reinforcement. In addition, higher degree of corrosion of lateral reinforcement in Group 3 caused the reduction in confinement effect of lateral reinforcement compared with Group 2 samples (see Table 4, the degree of corrosion of lateral reinforcement of group 2 and 3 were in the range of 5.31 to 7.38% and 8.23 to 11.62%, respectively. Similar to G2, the ductility of the confined concrete

and RC concrete columns was increased as a result of the improvement of strain at peak stress.

3.7. Failure modes and cracking patterns

For unconfined concrete (Group G1), when the load was small there was no cracking. As the load increased an initial crack appeared at the end of column and developed towards the central areas. The cracks widened until crushing of concrete at failure loads. The fly ash had no effect on the cracking pattern and failure modes of unconfined samples, and all four samples failed under slant shear cracking (see Fig. 13(a)).

For Group 2 (3V), fly ash improved the corrosion resistance of the lateral reinforcement leading to the improvement of the confinement effect. Fig. 13(b) shows the cracking pattern and failure modes of Group 2 samples where 3V DC was used to accelerate the corrosion of lateral reinforcement. When the load was small, no cracking appeared on the surface of the RC columns. However, as the concrete stress increased, cracks appeared on the surface of columns with increasing load. Three specimens with fly ash replacement showed similar cracking patterns at failure modes as lateral expansion failure and cracks appeared around the lateral reinforcement after initiation and outward buckling of the longitudinal steel bars. However, for control samples without fly ash, cracks appeared at the failure load along the longitudinal reinforcement, and the longitudinal bars were buckled. The specimens failed under inclined slant shear where the confinement effect of the lateral reinforcement was reduced by the relatively high degree of corrosion (11.5%).

(a) Group samples G1 (plain)

(b) Group samples G2 (3V)

(c) Group samples G3 (6V)

Figure 13. Failure modes and cracking patterns of the three groups of samples

For Groups G3 (6V), there were no visible cracks on the surface of the RC column at low load. When the applied load increased the stress of the confined concrete also increased, resulting in cracking on the surface of the RC columns. Cracks appeared along the longitudinal steel bars when the

stress of the concrete was higher than that of the peak stress, followed by the outward buckling of the longitudinal bars. Failure of the RC columns started as the confined concrete between the ties crushed. The failure of all four specimens was due to the combined lateral expansion and slant shear in which the lateral expansion was more dominant for sample S70.0.6.

4. Conclusions

The paper presents an experimental study on the combined effect of fly ash on the corrosion resistance of lateral reinforcement and stress-strain responses of confined concrete in RC columns. Based on the results reported in this paper, the following conclusions can be made:

- Within the scope of this study, fly ash improves the corrosion resistance of lateral reinforcement in RC columns. The greater the replacement of fly ash, the better the corrosion resistance due to a lower corrosion current density passing through the lateral reinforcement. As a result, fly ash decreases the degree of corrosion of lateral reinforcement and enhances the confinement effect under corrosion attack at 96 days.

- Lateral reinforcement shows less localised corrosion in specimens with higher fly ash replacements. Fly ash reduces the corrosion current density passing through the lateral reinforcement resulting in less localised corrosion.

- Fly ash increases the peak stress and corresponding strain at peak stress of confined concrete under accelerated corrosion of lateral reinforcement. Within the scope of this study, the best improvement in the stress-strain curve for confined concrete was when fly ash was used to replace OPC at a proportion of less than 20%. These increases are around 10% for peak stress and 92% for strain at peak stress when 6V DC corrosion acceleration was applied.

- The ductility of fly ash specimens is improved for both unconfined and confined concrete under accelerated corrosion of lateral reinforcement.

- Further research will be conducted on the wide range of parameters affecting the corrosion resistance and confinement effect of lateral reinforcement. These include bar diameter, spacing of lateral reinforcement, concrete compressive strength and, fly ash replacement proportions.

Acknowledgment

This work was supported by The University of Danang – University of Science and Technology, code number of Project: T2025-02-17.

References

[1] Bousalem, B., Chikh, N. (2007). Development of a confined model for rectangular ordinary reinforced concrete columns. *Materials and Structures*, 40(6):605–613.

[2] Nguyen, C. V. et al. (2025). Effect of square lateral reinforcement on the stress strain of confined concrete considering the buckling effect of longitudinal steel bars: an experimental and comparative study. *Journal of Building Pathology and Rehabilitation*, 10(2):121.

[3] Chung, H.-S., Yang, K.-H., Lee, Y.-H., Eun, H.-C. (2002). Stress-strain curve of laterally confined concrete. *Engineering Structures*, 24(9):1153–1163.

[4] Mander, J. B., Priestley, M. J. N., Park, R. (1988). Theoretical stress-strain model for confined concrete. *Journal of Structural Engineering*, 114(8):1804–1826.

[5] Mander, J. B., Priestley, M. J. N., Park, R. (1988). Observed stress-strain behavior of confined concrete. *Journal of Structural Engineering*, 114(8):1827–1849.

[6] Considère, A. (1906). *Experimental researches on reinforced concrete*. McGraw Publishing Company.

[7] Richart, F. E., Brown, R. L. (1934). *An investigation of reinforced concrete columns*. University of Illinois.

[8] King, J. W. H. (1946). The effect of lateral reinforcement in reinforced concrete columns. *The Structural Engineer*, 24(7):355–388.

[9] King, J. W. H. (1946). Further notes on reinforced concrete columns. *The Structural Engineer*, 24(11): 609–616.
[10] Chan, W. (1955). The ultimate strength and deformation of plastic hinges in reinforced concrete frameworks. *Magazine of Concrete Research*, 7(21):121–132.
[11] Szulczynski, T., Sozen, M. A. (1961). *Load-deformation characteristics of concrete prisms with rectilinear transverse reinforcement*. Civil Engineering Studies SRS-224, University of Illinois, Urbana, IL.
[12] Roy, H. E., Sozen, M. A. (1963). *A model to simulate the response of concrete to multi-axial loading*. Civil Engineering Studies SRS-268, University of Illinois, Urbana, IL.
[13] Bresler, B., Gilbert, P. H. (1961). Tie requirements for reinforced concrete columns. *ACI Journal Proceedings*, 58(11):555–570.
[14] Pfister, J. F. (1964). Influence of ties on the behavior of reinforced concrete columns. *ACI Journal Proceedings*, 61(5):521–536.
[15] Scott, B. D., Park, R., Priestley, M. J. N. (1982). Stress-strain behavior of concrete confined by overlapping hoops at low and high strain rates. *ACI Journal Proceedings*, 79(1):13–27.
[16] Vallenas, J., Bertero, V. V., Popov, E. P. (1977). *Concrete confined by rectangular hoops and subjected to axial loads*. Report No. UCB/EERC-77/13, Earthquake Engineering Research Center, University of California, Berkeley, CA.
[17] Scott, B. D. (1980). Stress-strain relationships for confined concrete: rectangular sections. Master's thesis, University of Canterbury, Christchurch, New Zealand.
[18] Saatcioglu, M., Razvi, S. R. (1992). Strength and ductility of confined concrete. *Journal of Structural Engineering*, 118(6):1590–1607.
[19] Hoshikuma, J., Kawashima, K., Nagaya, K., Taylor, A. W. (1997). Stress-strain model for confined reinforced concrete in bridge piers. *Journal of Structural Engineering*, 123(5):624–633.
[20] Andisheh, K., Scott, A., Palermo, A. (2021). Effects of corrosion on stress-strain behavior of confined concrete. *Journal of Structural Engineering*, 147(7):04021087.
[21] Ahmadi, J., Shalchiyan, M. M., Habibnejad Korayem, A., Ranjbar Karimi, E. (2020). An experimental investigation into the effect of transverse reinforcement corrosion on compressive strength reduction in spirally confined concrete. *Iranian Journal of Science and Technology, Transactions of Civil Engineering*, 44:265–275.
[22] Goharrokhi, A., Ahmadi, J., Shayanfar, M. A., Shalchiyan, M. M. (2020). Effect of transverse reinforcement corrosion on compressive strength reduction of stirrup-confined concrete: an experimental study. *Sādhanā*, 45:1–9.
[23] Vu, N. S., Yu, B., Li, B. (2017). Stress-strain model for confined concrete with corroded transverse reinforcement. *Engineering Structures*, 151:472–487.
[24] Zhang, G., Cao, X., Fu, Q. (2016). Experimental study on residual strength of concrete confined with corroded stirrups. *Canadian Journal of Civil Engineering*, 43(6):583–590.
[25] Gjorv, O. E. (1995). Effect of condensed silica fume on steel corrosion in concrete. *ACI Materials Journal*, 92(6):591–598.
[26] Cao, H., Sirivivatnanon, V. (1991). Corrosion of steel in concrete with and without silica fume. *Cement and Concrete Research*, 21(2–3):316–324.
[27] Hossain, K. M. A., Lachemi, M. (2004). Corrosion resistance and chloride diffusivity of volcanic ash blended cement mortar. *Cement and Concrete Research*, 34(4):695–702.
[28] Saraswathy, V., Muralidharan, S., Thangavel, K., Srinivasan, S. (2003). Influence of activated fly ash on corrosion-resistance and strength of concrete. *Cement and Concrete Composites*, 25(7):673–680.
[29] Shaikh, F. U. A., Supit, S. W. M. (2015). Compressive strength and durability properties of high volume fly ash (HVFA) concretes containing ultrafine fly ash (UFFA). *Construction and Building Materials*, 82: 192–205.
[30] Van Nguyen, C., Lambert, P., Hung Tran, Q. (2019). Effect of Vietnamese fly ash on selected physical properties, durability and probability of corrosion of steel in concrete. *Materials*, 12(4):593.
[31] Tittarelli, F., Mobili, A., Bellezze, T. (2017). The effect of fly ash on the corrosion behaviour of galvanised

steel rebars in concrete. In *IOP Conference Series: Materials Science and Engineering*, IOP Publishing.

[32] Choi, Y.-S., Kim, J.-G., Lee, K.-M. (2006). Corrosion behavior of steel bar embedded in fly ash concrete. *Corrosion Science*, 48(7):1733–1745.

[33] Ha, T.-H., Muralidharan, S., Bae, J.-H., Ha, Y.-C., Lee, H.-G., Park, K.-W., Kim, D.-K. (2007). Accelerated short-term techniques to evaluate the corrosion performance of steel in fly ash blended concrete. *Building and Environment*, 42(1):78–85.

[34] Montemor, M. F., Simões, A. M. P., Salta, M. M. (2000). Effect of fly ash on concrete reinforcement corrosion studied by EIS. *Cement and Concrete Composites*, 22(3):175–185.

[35] Van Nguyen, C., Lambert, P., Bui, V. N. (2020). Effect of locally sourced pozzolan on corrosion resistance of steel in reinforced concrete beams. *International Journal of Civil Engineering*, 18(6):619–630.

[36] TCVN 10302:2014 (2014). *Activity admixture – Fly ash for concrete, mortar and cement*. Vietnam Standards and Quality Institute, Hanoi, Vietnam.

[37] Nguyen, C. V., Lambert, P. (2018). Effect of current density on accelerated corrosion of reinforcing steel bars in concrete. *Structure and Infrastructure Engineering*, 14(11):1535–1546.

[38] O'Flaherty, F. J., Mangat, P. S., Lambert, P., Browne, E. H. (2008). Effect of under-reinforcement on the flexural strength of corroded beams. *Materials and Structures*, 41:311–321.

[39] Lambert, P., Nguyen, C. V., Mangat, P. S., O'Flaherty, F. J., Jones, G. (2015). Dual function carbon fibre fabric strengthening and impressed current cathodic protection (ICCP) anode for reinforced concrete structures. *Materials and Structures*, 48:2157–2167.

[40] Nguyen, C. V., Lambert, P., Mangat, P. S., O'Flaherty, F. J., Jones, G. (2016). Near-surface mounted carbon fibre rod used for combined strengthening and cathodic protection for reinforced concrete structures. *Structure and Infrastructure Engineering*, 12(3):356–365.

[41] Sun, Y., Lee, H. S. (2022). Effect of fly ash with or without mechanical activation on early-age cement hydration: A comparative case study by boundary nucleation and growth model. *Thermochimica Acta*, 716:179306.

[42] Akmalaiuly, K., Berdikul, N., Alex, A. G., Negim, E.-S. (2023). The effect of mechanical activation of fly ash on cement-based materials hydration and hardened state properties. *Materials*, 16(8):2959.

[43] Dhakal, R. P., Maekawa, K. (2002). Path-dependent cyclic stress-strain relationship of reinforcing bar including buckling. *Engineering Structures*, 24(11):1383–1396.